Journal of Physiology (1989), **417**, *pp.* 25–51
With 14 *text-figures*
Printed in Great Britain

INHIBITORY INTERACTIONS BETWEEN MOTONEURONE TERMINALS IN NEONATAL RAT LUMBRICAL MUSCLE

BY W. J. BETZ*, M. CHUA* AND R. M. A. P. RIDGE†

*From the *Department of Physiology, University of Colorado School of Medicine, Denver, CO 80220, USA, and the †Department of Physiology, University of Bristol School of Medical Sciences, University Walk, Bristol BS8 1TD*

(*Received 9 March 1989*)

SUMMARY

1. Evoked synaptic potentials and currents were recorded in neonatal rat fourth deep lumbrical muscle during the period of polyneuronal innervation. Signs of inhibitory interactions between converging mononeurone terminals were detected.

2. Muscle fibres innervated by axons from the lateral plantar nerve (LPN) and from the sural nerve (SN) were studied. In unblocked preparations the muscle contracted, and electrode tips were mounted on flexible wires to prevent loss of impalements.

3. In voltage recordings from unblocked preparations, paired two-shock stimulation of one nerve revealed synaptic depression: the second response was smaller than the first. When the two stimuli were delivered to different nerves (SN and LPN), the second response was smaller than its own control.

4. In voltage clamped, unblocked preparations, a similar result was obtained. Conditioning stimulation of one nerve (SN, for example) inhibited the response to test stimulation of the other nerve (LPN). The inhibition was greater with larger conditioning responses, was maximal when the conditioning and test stimuli were approximately superimposed, and decayed with a time course of several tens of milliseconds. Several tests showed that the end-plate was well clamped; the observed inhibition could not be explained by voltage escape at the end-plate.

5. The inhibition was not constant during the tail of the test end-plate current (EPC). Instead, it declined during the EPC tail, suggesting that the mechanism of inhibition was active, though diminishing, throughout the time course of the test EPC.

6. The amount of inhibition was not noticeably affected by altering the muscle membrane potential (two cells studied).

7. Treatment with curare or α-bungarotoxin to block most ACh receptors reduced the inhibition. In about half of the fibres studied, no inhibition was evident; in the others, up to 50% inhibition was observed. The average inhibition for all receptor-blocked fibres was about 15%.

8. In six α-bungarotoxin-treated cells, multiple conditioning stimuli were

† To whom all correspondence should be addressed.

MS 7570

delivered. In most cases, the amount of inhibition increased with increasing numbers of conditioning stimuli.

9. Several possible mechanisms of inhibition are discussed, including reduction of current through ACh channels during the test response owing to alterations in synaptic cleft ion concentrations produced by the conditioning response, presynaptic inhibition of transmitter release, and postsynaptic receptor saturation.

INTRODUCTION

During development of vertebrate skeletal muscle, axons from several different monotoneurones converge at each end-plate. Electron micrographs of developing mammalian neuromuscular junctions (Bixby, 1981) show that terminal profiles lie in close apposition, often without intervening Schwann cell processes. Light microscopic visualization of individual nerve terminal arborizations in adult frog (Werle & Herrera, 1987) and embryonic snake (Lichtman, Wilkinson & Rich, 1985) show varying degrees of terminal interdigitation, with terminals from different axons often lying in close physical proximity. This close contact between terminals raises the possibility of physiological interactions between terminals, either through pre- or postsynaptic mechanisms. We have detected signs of such interactions using electrophysiological techniques and a simple experimental protocol.

We used the neonatal rat lumbrical muscle, which receives its motor input from two different peripheral nerves. Most axons arrive via the lateral plantar nerve (LPN); a few arrive via the sural nerve (SN). We impaled muscle fibres at their end-plate and then stimulated the two nerves separately to identify fibres innervated by axons in both nerves (Betz, Caldwell & Ribchester, 1979). We then recorded end-plate currents (EPCs) in response to individual nerve stimulation (control) and to paired stimulation. We found that when both nerves were stimulated within about 50 ms of each other the second EPC was reduced relative to its control amplitude. Further experiments suggested that changes in ion concentrations in the synaptic cleft as a consequence of postsynaptic activity may inhibit transmitter release or action, although other mechanisms may be involved additionally. Some of these results have been presented in preliminary form (Betz, Chua & Ridge, 1989).

METHODS

All experiments were performed on fourth deep lumbrical muscles dissected together with their nerve supply from 4- to 9-day-old rats, which were killed by stunning and decapitation. Both the sural nerve (SN) and lateral plantar nerve (LPN) supply motor innervation to the muscle; the separate nerves join near the heel (Betz *et al.* 1979). About 20% of the polyneuronally innervated neonatal muscle fibres receive inputs from both nerves; in each such muscle fibre, SN and LPN inputs converge at a single end-plate. Thus, by stimulating the nerves separately and together we could study interactions between the two.

Nerve–muscle preparations were pinned in a small, Sylgard-lined dish and the SN and LPN were drawn into separate suction stimulating electrodes. The preparation was continuously superfused with Krebs solution of the following composition (mM): NaCl, 136; KCl, 5; $MgCl_2$, 1; PIPES buffer 2; glucose 11. $CaCl_2$ was raised from a normal 2 mM concentration to 6 or 8 mM to improve the quality of microelectrode penetrations. Solutions were bubbled with 100% O_2. All experiments were performed at room temperature (20–22 °C). In some experiments acetylcholine (ACh) receptors were blocked with *d*-tubocurarine or α-bungarotoxin. *d*-Tubocurarine was added to the

perfusion medium; the concentration was usually 3 μM-α-bungarotoxin (1 μg/ml) was added to the perfusing medium temporarily, while monitoring end-plate potentials (EPPs) in a muscle fibre. At the first sign of reduction in EPP amplitude, the α-bungarotoxin concentration was reduced to 0·5 or 0·25 μg/ml; when the EPP had declined to a low level (2–5 mV), perfusion of toxin-free medium was begun again. It was considerably more difficult to achieve an appropriate block level with α-bungarotoxin than with *d*-tubocurarine, since the concentration of the latter could be adjusted during the experiment if necessary.

Most experiments were performed on unblocked preparations. Thus, when either nerve was stimulated, the muscle contracted. To avoid dislodging intracellular microelectrodes, muscles were stretched to about 120% of their resting length and 'floating' microelectrode tips were used. These were made by scoring and then breaking off, under water, the tip (1–2 mm long) of conventional microelectrodes. The tip was then mounted on a highly compliant, coiled silver wire; a dab of Vaseline held the tip to the wire. With this arrangement, some penetrations were held long enough to record dozens, and in some cases hundreds, of synaptic responses.

Stimuli were delivered independently to SN and LPN from a WPI stimulator with isolated outputs. The usual protocol involved stimulating each nerve separately at 15–60 s intervals, and then paired at a short interval (0–100 ms). Each of the three traces was stored for later analysis. This cycle was repeated a number of times before changing the interval or other parameters; such a repeated cycle is referred to as a run. Recordings were displayed on a Nicolet Explorer oscilloscope. Digitized data were stored on magnetic disc and analysed with a Hewlett-Packard 9816 computer. An Axoclamp IIA amplifier (Axon Instruments) was used for all recordings and both single- and two-electrode voltage clamping. Membrane currents were measured from the current applied to the feedback circuit.

Single-electrode voltage clamp

Initially, we tried to use the single-electrode voltage clamp (SEVC) technique to clamp the muscle membrane potential. In most experiments the following parameters applied: electrode resistance, 20–30 MΩ; feedback gain, 8 nA/mV; time constant, 2 ms; switching frequency, 8–15 kHz. Muscle fibre input resistance was usually 10–30 MΩ, but could be as high as 100 MΩ. The voltage on the electrode was carefully monitored. Under these conditions it appeared that the SEVC was working well; voltage escape at the peak of the EPC appeared to be only a few millivolts. However, a further check with a second, independent recording electrode revealed serious voltage escape at the impalement site in the SEVC mode. We then switched to conventional two-electrode voltage clamp (TEVC) and repeated the observations. Results are shown in Fig. 1. Superimposed traces (Fig. 1*A*) show EPCs obtained at different membrane potentials for two-electrode clamping (left side) and SEVC (right side). Both techniques gave similar passive *I–V* curves (Fig. 1*B*), but the SEVC greatly underestimated EPC amplitude (Fig. 1*C*). Thus, we abandoned the SEVC technique.

Conventional voltage clamp

The need to use two intracellular microelectrodes added significantly to the technical difficulty of the experiments. Obtaining good resting potentials with both electrodes precisely localized at the end-plate and maintaining stable impalements while the muscle contracted was tedious; our success rate was low, with about 90% of the fibres lost or discarded before useful data could be obtained. A number of criteria (described later) were developed to check the integrity of the data. The two-electrode clamp worked well. A typical record is shown in Fig. 2. EPPs are shown in Fig. 2*A*; the smaller was obtained under voltage clamp and is enlarged in Fig. 2*B*. The clamped EPC is shown in Fig. 2*C*. The maximum voltage escape was less than 2 mV and this occurred during the initial part of the EPC; at the peak of the EPC, the voltage escape was less than 0·5 mV.

In some experiments, we used the dye 4-Di-2-ASP (4-(4-diethylaminostyryl)-*N*-methylpyridinium iodide; supplied by Molecular Probes, Inc., Eugene, OR, USA; Magrassi, Purves & Lichtman, 1987) to stain nerve terminals. Krebs solution containing the dye (5 μM) was perfused through the chamber for 1 min; the preparation was then observed in ultraviolet light with a Leitz epifluorescence microscope. Observation periods had to be kept short to avoid photo-damage to the nerve terminals, indicated by a rise in miniature end-plate potential (MEPP) frequency. Thus, we used this procedure to observe surface fibres briefly and visually localize small clusters of end-plates. Fibres were then impaled while illuminated with transmitted visible light.

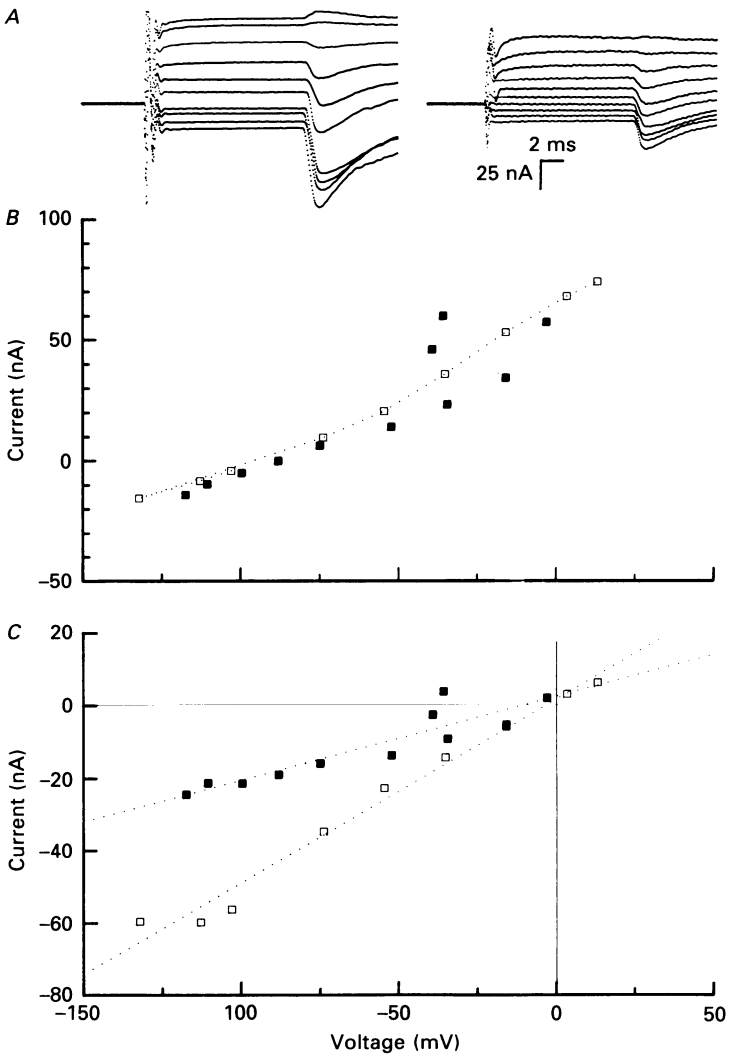

Fig. 1. Comparison of single-electrode voltage clamp (SEVC) and two-electrode voltage clamp (TEVC) in the same cell. *A*, superimposed records of EPCs with the membrane potential clamped to different levels. TEVC (left) and SEVC (right) traces are shown. Analyses of these data are shown in *B* and *C* for TEVC (□) and SEVC (■). *B*, passive membrane *I–V* curves are similar for the two modes of clamping. Measurements were made 1 ms before the EPC deflection. *C*, EPC amplitudes were seriously underestimated in SEVC mode, owing to large amounts of voltage escape.

RESULTS

Voltage recordings, unblocked preparations

Repetitive stimulation of a single input

Use-dependent changes in the amplitude of synaptic potentials have been described in a variety of preparations. At the neuromuscular junction, presynaptic

changes in transmitter release (e.g. facilitation, depression, post-tetanic potentiation) and altered postsynaptic responsiveness (e.g. non-linear voltage summation) have been shown to contribute to changes in EPP amplitude with repetitive activity (see Erulkar, 1983, for review). As illustrated in Fig. 3*A*, in neonatal muscle we observed

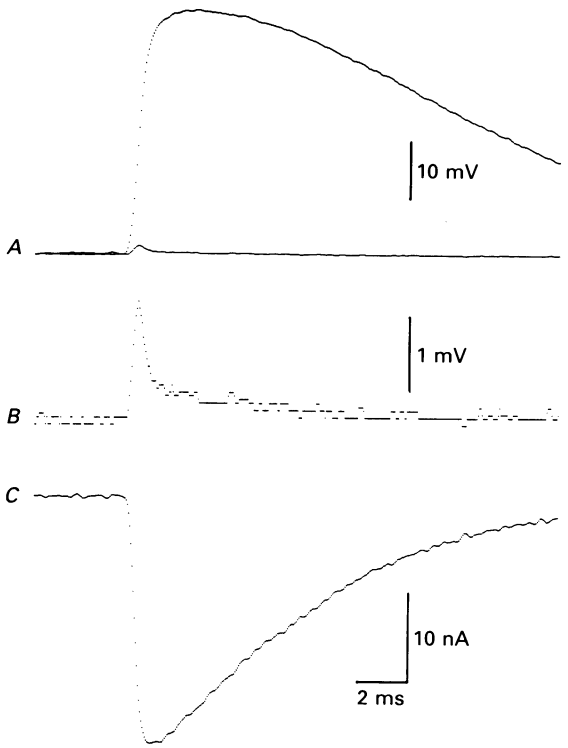

Fig. 2. Conventional (two-electrode) voltage clamp operated at over 97% efficiency. *A*, unclamped (upper trace) and clamped (lower trace) EPP. *B*, clamped EPP at higher gain. *C*, EPC under voltage clamp. Note that the maximum voltage escape was about 1·5 mV, and that at the peak of the EPC the voltage escape was less than 0·5 mV. Membrane clamped at resting potential (−51 mV).

a reduction in the amplitude of a test EPP which followed a conditioning EPP, with both stimuli delivered to the same nerve; twelve superimposed sweeps are shown in Fig. 3*A*. At short conditioning–test intervals, when the test response rose from the tail of the conditioning EPP, the test EPP amplitude was greatly reduced. Since test EPPs arose from the tail of the conditioning EPP, part of this reduction can be attributed to non-linear summation of voltage. This cannot be the complete explanation, however, since at short intervals the peaks of the test EPPs do not reach the same membrane potential as control EPP peaks. Other factors, such as a reduction in transmitter release (synaptic depression) and/or an increase in postsynaptic membrane conductance, could also contribute to the observed reduction in test EPP amplitude.

Interactions between separate inputs

Figure 3*B* shows results from a different kind of experiment in which the conditioning and test stimuli were delivered to separate axons innervating the same end-plate. In such cases the test response was compared not to the conditioning

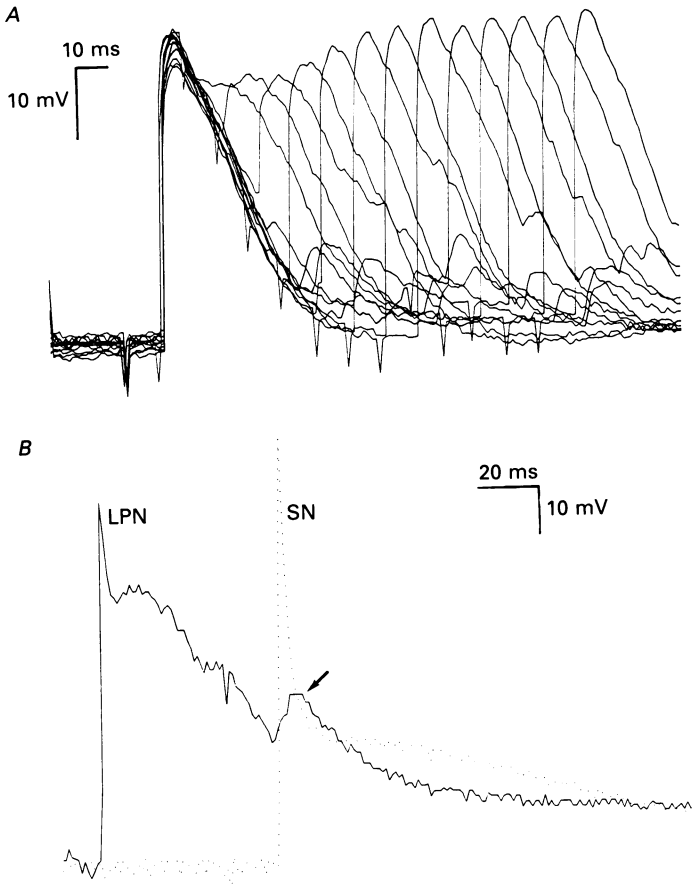

Fig. 3. *A*, two-shock stimulation of a single input. At 10 s intervals the LPN was stimulated twice, the intershock interval varying in 10 ms increments. The superimposed traces show that the second response of the pair was depressed if it occurred at a short interval, particularly during the decay phase of the first response. Membrane potential, −48 mV. *B*, interaction between LPN and SN. In this unblocked preparation, SN stimulation alone produced an action potential (dotted trace). The response was much smaller (arrow) if it was preceded by LPN stimulation. Resting potential, −71 mV.

response, but to its own control, recorded in the absence of conditioning stimulation. The usual procedure was to evoke in turn at 10 s intervals conditioning, control, and then conditioning–test responses, with the conditioning–test interval fixed. This cycle was repeated a number of times, and responses were averaged in most cases. Such a series constituted one run. In some cells, it was possible to record several runs

under different conditions (e.g. different conditioning–test intervals). In Fig. 3*B*, stimulation of the sural nerve (SN) alone produced an action potential. If however, SN stimulation followed lateral plantar nerve (LPN) stimulation by a short interval, the SN response was greatly diminished. This reduction has a trivial explanation, namely that the SN test response arose during the muscle fibre's refractory period.

Another example of interaction between SN and LPN is shown in Fig. 4. In this cell, action potentials were not observed, owing to the relatively depolarized membrane potential (−54 mV). Averaged responses at three different conditioning (LPN)−test (SN) intervals are shown in Fig. 4*A*. In each case, the SN test EPP was smaller than its control. (Each test EPP amplitude was measured from the extrapolated tail of the conditioning EPP. In many experiments, conditioning responses were recorded without test responses to check that the extrapolations were accurate.) Results are plotted in Fig. 4*B* (□), where percentage inhibition is defined as $100\,(1-V_{\text{test}}/V_{\text{control}})$.

Again, non-linear voltage summation cannot account fully for the observed inhibition, because the peaks of the test EPPs did not reach the same membrane potential as their controls (Fig. 4*A*). In fact, correcting for non-linear summation increases, rather than decreases the amount of inhibition (Fig. 4*B*, △). Clearly, some other mechanism(s) must be contributing to the inhibition. Presynaptic use-dependent effects, however, cannot be involved here, since the conditioning stimulus was given to LPN, and the test stimulus to SN.

Results from fourteen cells (thirty-six runs) in which this type of experiment (unblocked preparation, voltage recording) was performed are shown in Fig. 4*C*. Most cells showed inhibition, which lasted a few tens of milliseconds and had fully decayed within about 100 ms. In general, the inhibition was reciprocal in that the response to either nerve was inhibited if preceded by stimulation of the other nerve. The amount of inhibition also depended upon the size of the conditioning EPP, with larger EPPs giving more inhibition.

Voltage clamp, unblocked preparations

The large postsynaptic voltage changes produced by conditioning EPPs could easily produce conductance changes which could reduce the amplitude of a subsequent test EPP. In order to prevent such postsynaptic changes, voltage clamp experiments were performed (see Methods). Clear signs of inhibitory interactions were still observed with voltage clamping. Examples are shown in Figs 5 and 6. Figure 5*A* shows superimposed averaged EPCs in response to LPN stimulation (control) and SN–LPN (conditioning–test) stimulation. It is clear that the current produced by LPN stimulation was reduced when it was preceded by conditioning SN stimulation by several milliseconds. Results from another run are shown in Fig. 5*B*. Stimulation of SN or LPN alone produced (averaged) EPCs of about 20 nA in amplitude; stimulation of both nerves so that the EPC peaks approximately coincided (Both) produced a marginally larger EPC, far less than the expected sum of individual responses. Measured against control SN, the observed inhibition was 80%; against control LPN, the inhibition was 67%. A total of seven such runs were obtained from this cell. SN was stimulated first in some runs (e.g. Fig. 5*A*); in other runs, LPN was stimulated first. Figure 5*C* shows the percentage inhibition for all

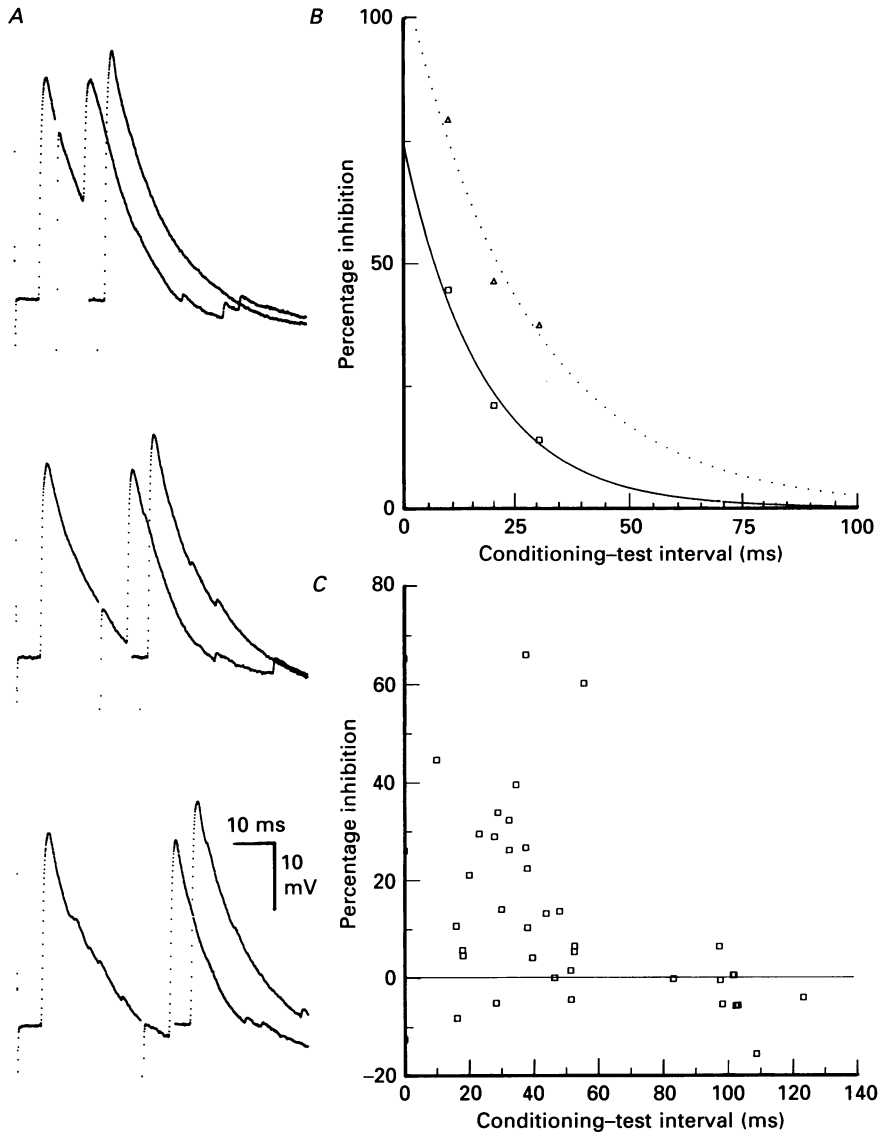

Fig. 4. Interaction between LPN and SN. Action potentials were not observed in this unblocked cell, probably owing to the relatively low resting potential (−54 mV). *A*, averaged EPPs. The peaks, left to right, are LPN (conditioning), SN (test), and SN (control, offset slightly to the right for clarity). The LPN–SN interval was 10 ms (top traces), 20 ms (middle) and 30 ms (bottom). Note that each SN test response, measured from the extrapolated tail of the LPN response, was smaller than its control. Moreover, the peak of each SN test response did not reach the same membrane potential as the peak of the control response. *B*, the percentage inhibition, defined as $100\,(1 - V_{test}/V_{control})$ where V_{test} is the peak amplitude of the test EPP (measured from the extrapolated tail of the conditioning EPP) and $V_{control}$ is the peak amplitude of control EPP, is plotted against conditioning–test interval. □, raw data; △, data in which each EPP was corrected for non-linear voltage summation before averaging. Lines are best exponential fits (method of linear least squares). *C*, data from all unblocked preparations in which control responses did not give action potentials (fourteen cells; thirty-six runs).

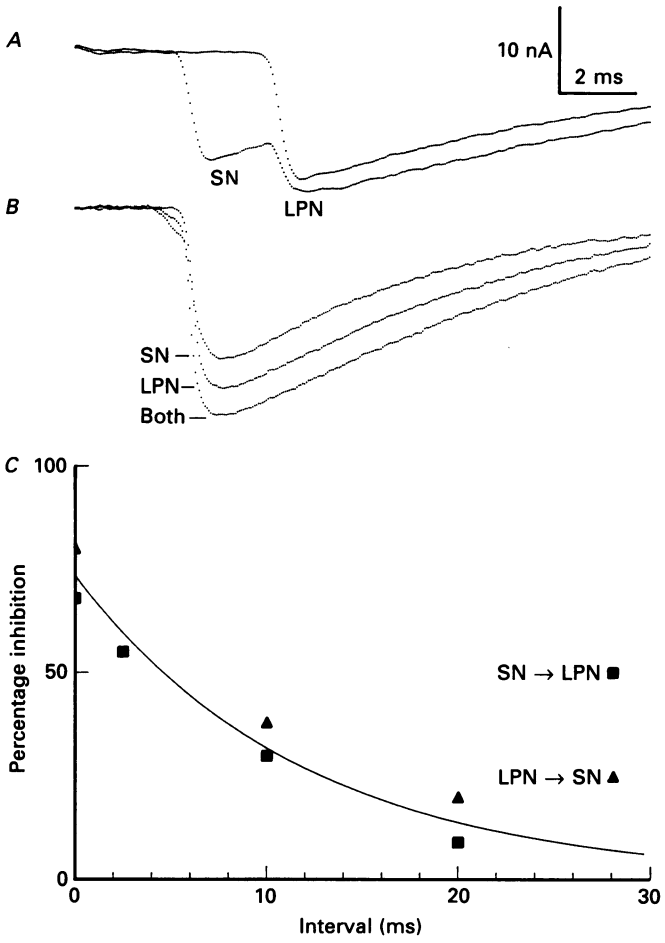

Fig. 5. Interaction produced by LPN and SN stimulation in unblocked preparation under voltage clamp. *A*, inhibition of LPN by SN. The LPN test response (measured from the extrapolated tail of the SN response) was smaller than the LPN control response. *B*, simultaneous stimulation of LPN and SN produced a response (Both) which was larger than either SN or LPN alone, *but much smaller than the sum of the two individual responses.* EPCs in *A* and *B* are averages of three to six individual responses. *C*, results of seven runs in the same cell at different intervals with SN (■) or LPN (▲) as conditioning stimulus. The line is an exponential best fit to all points.

runs, plotted against the conditioning–test interval. The line is an exponential best fit for all points. The inhibition in this cell was maximal when the two responses were approximately superimposed. The inhibition of SN by LPN was slightly larger than the reverse (inhibition of LPN by SN); this parallels the size of the individual EPCs. In fact, in this and all other experiments, the larger EPC produced the greater inhibition, as was the case for voltage recordings described above.

Figure 6 shows another example of the inhibition observed under voltage clamp conditions. In this cell, multiple EPCs were observed with LPN or SN stimulation, suggesting that each nerve supplied more than one axon to the muscle. The averaged EPCs in response to supramaximal stimulation are shown in Fig. 6*A*. In Fig. 6*B* the

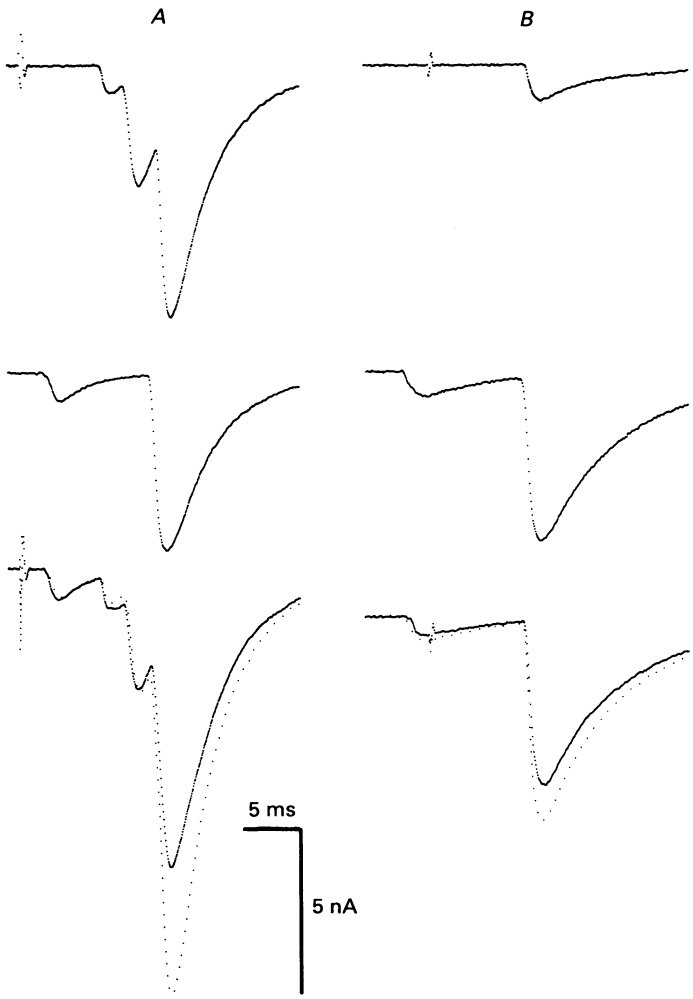

Fig. 6. In this cell, the muscle fibre was innervated by more than one axon in both LPN and SN. *A*, stimulation of SN alone (top) or LPN alone (middle) produced multiple EPCs, indicating that several axons from each nerve innervated the fibre. In the bottom trace, both nerves were stimulated simultaneously. The dotted curve at the bottom shows the arithmetic sum of the top and middle traces. *B*, same cell and protocol as in *A*, except that the SN stimulus was reduced in amplitude and delivered later (compare top traces in *A* and *B*). All traces are averages of three to six EPCs.

stimulus to the SN was reduced so that a single deflection was observed (compare top traces in *A* and *B*). In both cases, stimulation of both nerves produced a smaller response than the sum of the responses to separate stimulation of each nerve.

Spontaneous miniature EPCs were also observed on many traces, and allowed us

to calculate quantal content of the evoked EPCs. In most cells, quantal content fell between 8 and 20 quanta. For example, in the cell illustrated in Fig. 5, miniature EPCs averaged −2·4 nA in amplitude (recorded at a −91 mV holding potential; S.D., 1·0 mV; $n = 21$). This gives a quantal content for LPN of 19 and for SN of 16.

In summary, the observed inhibition was maximal at or close to zero separation, was larger for larger conditioning EPCs, and decayed with a time constant that was similar to the decay of the conditioning EPC.

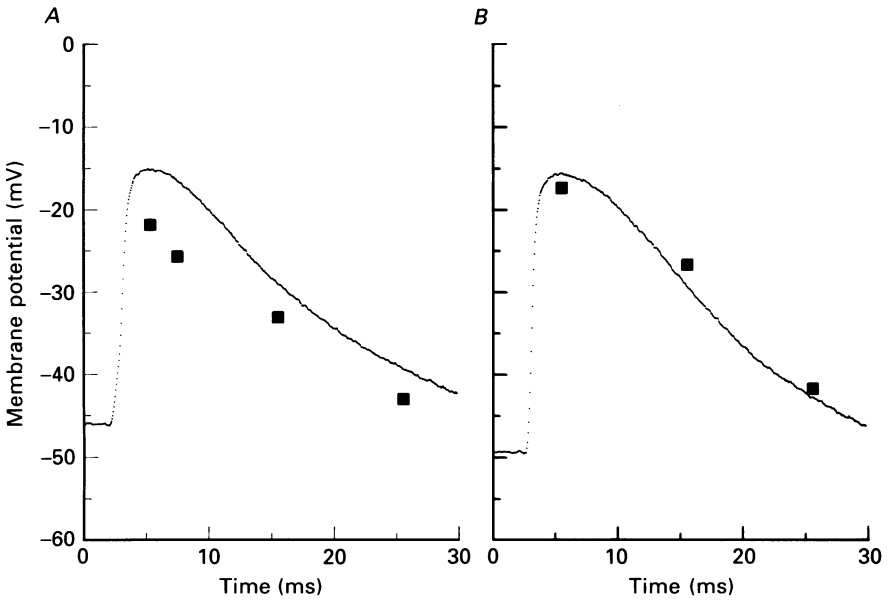

Fig. 7. Traces show end-plate potentials in response to SN (*A*) or LPN (*B*) stimulation. The squares show, for each of the seven runs under voltage clamp, the amount of voltage escape at the end-plate which would be required to explain the inhibition of the test response of one nerve by conditioning stimulation of the other nerve. Much, and in some cases all, of the unclamped EPP would have to escape clamping in order to explain fully the observed inhibition.

All of these observations could be explained if the efficiency of the voltage clamp was inadequate. While there is little doubt that the voltage was well controlled at the site of impalement (see Methods), if the impalements were not precisely at the end-plate, serious voltage escape at the end-plate could produce effects like those we observed. That is, voltage escape at the end-plate during the conditioning response would reduce the driving force for inward current during the test response, thereby producing apparent inhibition of the test EPC. To estimate how inadequate the clamp would have to be, we calculated the amount of voltage escape at the end-plate that would have had to occur in order to explain the observed inhibition. For example, if we observed 40% inhibition of the test EPC, it would require a depolarization at the end-plate sufficient to reduce the electrical driving force by 40% to explain fully the observed inhibition. Results from the cell of Fig. 5, which are typical of other cells, are shown in Fig. 7. The traces show unclamped EPPs in response to SN and LPN stimulation. The squares mark the voltage change at the

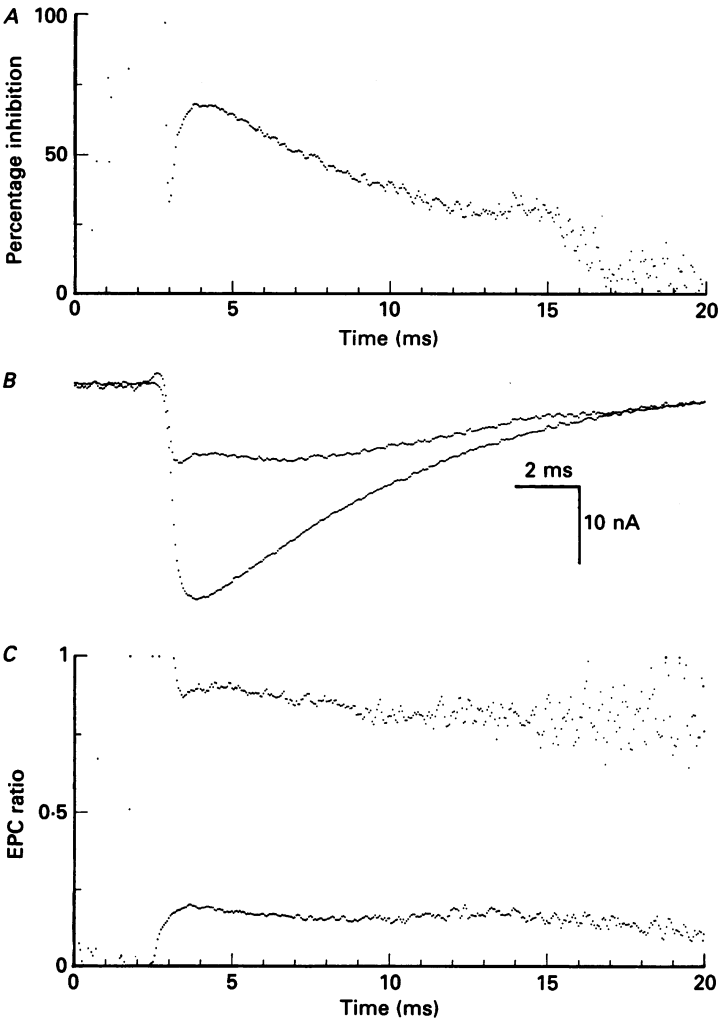

Fig. 8. Decay of inhibition during the decay of the test EPC. Inhibition calculated as in Fig. 4. *A*, for the traces in Fig. 5*B*, the percentage inhibition was calculated for every point during the decay of the test EPC. Note that the inhibition decreased during the decay. *B*, for the same data, the lower trace is the LPN EPC; the upper trace is the response to simultaneous stimulation of LPN and SN (marked Both in Fig. 5*B*) minus the SN response. In other words, the upper trace is the amount added to the SN response by simultaneous LPN stimulation. Its rather flattened time course during the decay of the LPN response gives rise to the decay of inhibition during the EPC tail. *C*, to test whether large EPCs decay faster or slower than small EPCs, two EPC amplitude ratios are plotted. The upper trace is the ratio of SN/LPN for the data in *A* and *B*. The lower trace shows the SN/LPN ratio from a different experiment (Fig. 6*B*). The ratios show a small decrease over time, indicating that small EPCs decayed only slightly faster than larger EPCs. This cannot account for the decay of inhibition during the tail of test EPCs.

end-plate which would be needed to explain fully the observed inhibition in each of the seven runs performed on this cell (ACh reversal potential assumed to be −10 mV). It is clear that a very poor clamping efficiency would be required; over 70%, and in some cases over 95%, of the EPP at the end-plate would have to escape from the voltage clamp to produce the observed inhibition.

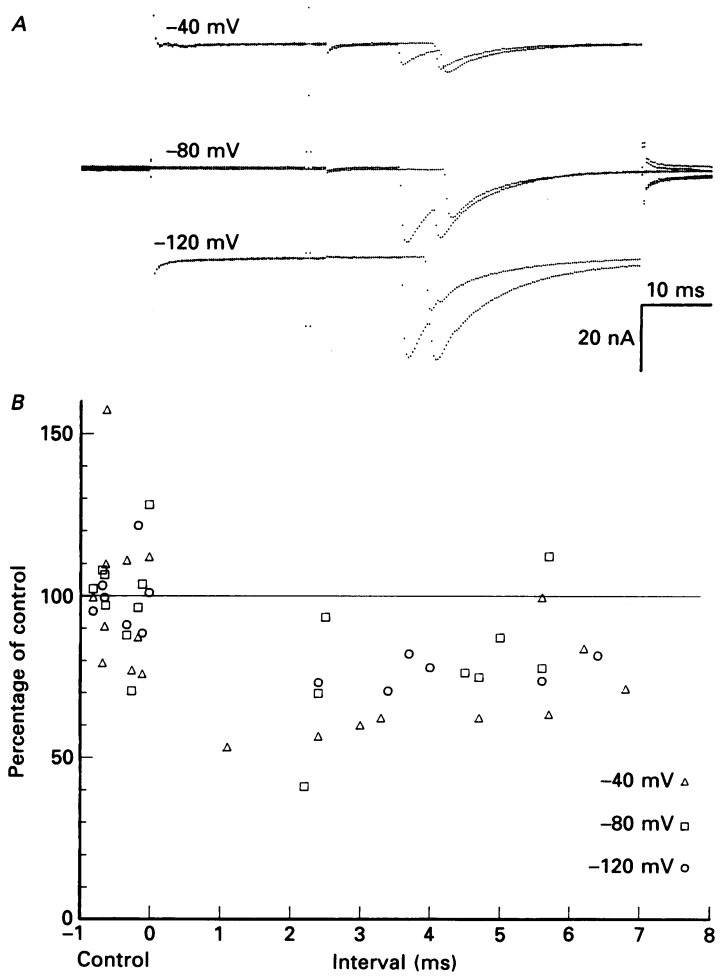

Fig. 9. Clamping to different membrane potentials had little effect on the amount of inhibition. The amount of inhibition was measured at −40, −80 and −120 mV. *A*, sample traces. A pair of superimposed traces (control and conditioning-test EPCs) is shown at each membrane potential. *B*, all results from this cell, with varying intervals between LPN and SN stimulation.

We conducted several independent tests to examine further the possibility of large amounts of voltage escape at the end-plate. The results of these tests are described below and in the Appendix. They strongly suggest that the observed inhibition cannot be explained by inadequate clamping at the end-plate.

Qualitative tests of voltage clamp efficiency

In some experiments we used 4-Di-2-ASP to localize end-plates visually. As described in the Methods, this procedure was used to localize small clusters of surface end-plates; fibres were then impaled under transmitted light. Thus, the technique did not allow us to localize individual end-plates with absolute precision, but helped us find the end-plate more easily.

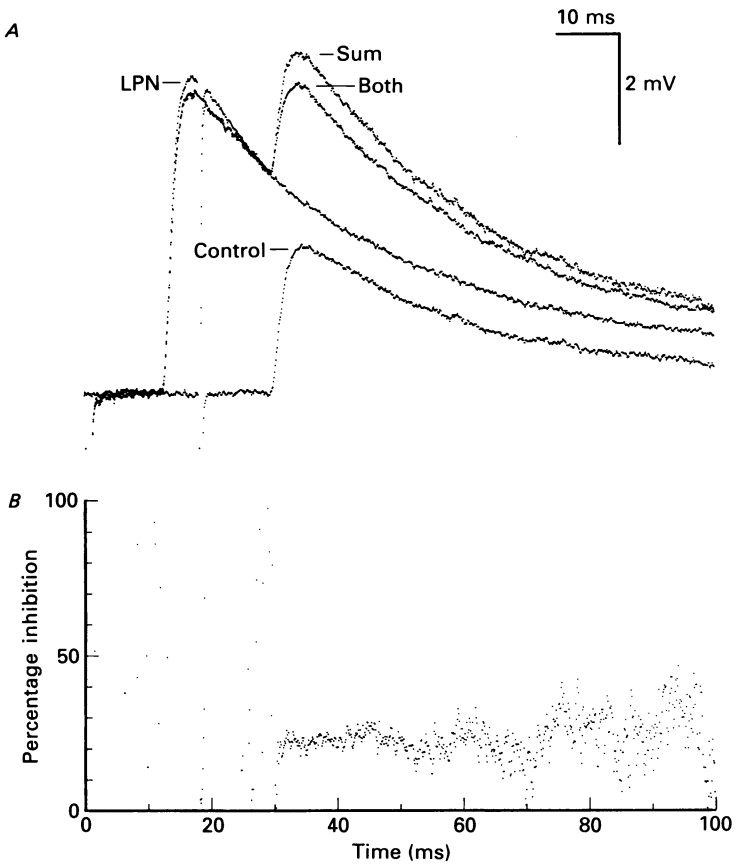

Fig. 10. Inhibition with most ACh receptors blocked by pre-treatment with α-bungarotoxin. *A*, averaged EPPs, showing that the test SN response (Both) was inhibited when preceded by a conditioning LPN response compared to control. The trace (Sum) shows the arithmetic sum of separate LPN and SN responses. *B*, the inhibition observed was nearly constant throughout the decay phase of the EPP. Resting potential, −56 mV. Non-linear voltage summation can account for only a few per cent of the observed inhibition.

We also compared the time courses of EPPs and EPCs; impalements at end-plates gave EPCs with decay time courses significantly shorter than EPP decays (See Fig. 2). A single exponential described most of the decay, but the time constants were very different (about 9 ms for EPC, 19 ms for EPP). The much faster EPC decay is expected if the impalement is at the end-plate, since the EPC reflects transmitter action directly, while the EPP decay reflects this and, additionally, passive discharge

of membrane capacitance and voltage-sensitive conductance changes. Impalements remote from the end-plate gave EPCs and EPPs with decay time courses which were very similar to each other.

We also measured passive and active *I–V* relationships and EPC reversal potential

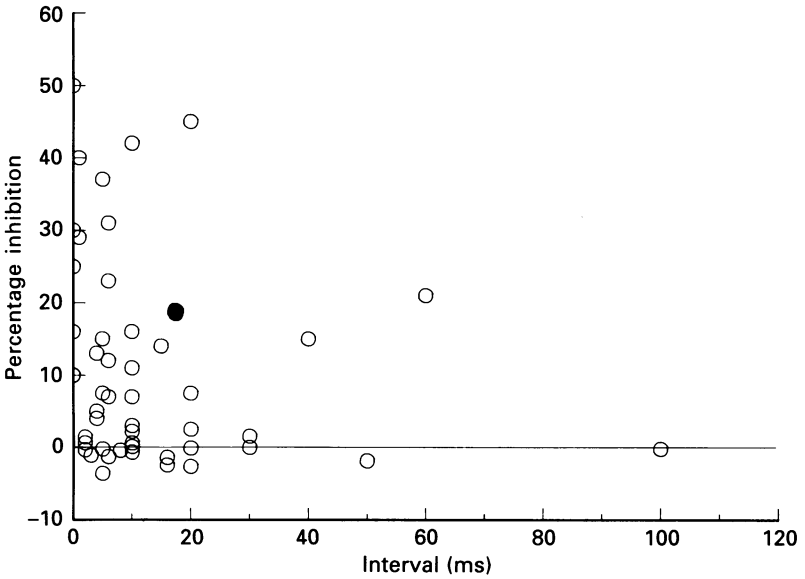

Fig. 11. Summary of all results in α-bungarotoxin-treated preparations. All responses were corrected for non-linear voltage summation assuming a reversal potential of −10 mV. The filled symbol represents the cell in Fig. 10.

in every cell (see Appendix). If the electrodes were remote from the end-plate, the EPC *I–V* relationship was not linear and the reversal potential shifted to positive values; such cells were discarded. This test was a sensitive indicator of proximity to the end-plate. Our initial criterion for proceeding with a cell was that the reversal potential be negative; after the experiment was completed, more stringent criteria were also applied. These are described in detail in the Appendix. Briefly, we estimated the maximum distance possible between the recording site and the end-plate, and concluded for the impalements we accepted that this distance was within 0·06 length constants. Finally, we calculated from this the maximum voltage escape that might have occurred in each cell, and found that this could not account fully for the observed inhibition.

Decay of inhibition during EPC tails

We next extended the analysis of inhibition from a consideration of peak EPC amplitudes to include the decay phases. For example, if the peak of a test EPC was inhibited by 40%, would the decay phase of the EPC also show 40% inhibition throughout its duration? Typical results are illustrated in Fig. 8, which shows that the inhibitory effect did decay during the tail of the test EPC. The data are from the experiment shown in Fig. 5*B*. In Fig. 8*A*, the percentage inhibition for each point in the EPC is defined as before: $100\ (1-I_{\text{test}})/I_{\text{control}})$. The peak of the EPCs occurred

at about 4 ms. During the decay phase of the test EPC, the amount of inhibition declined; the time course of the decay of inhibition was approximately the same as the decay of the EPC. This can also be seen in Fig. 8*B*. Here, the lower trace is the LPN EPC; the upper trace is the difference between the EPCs in response to

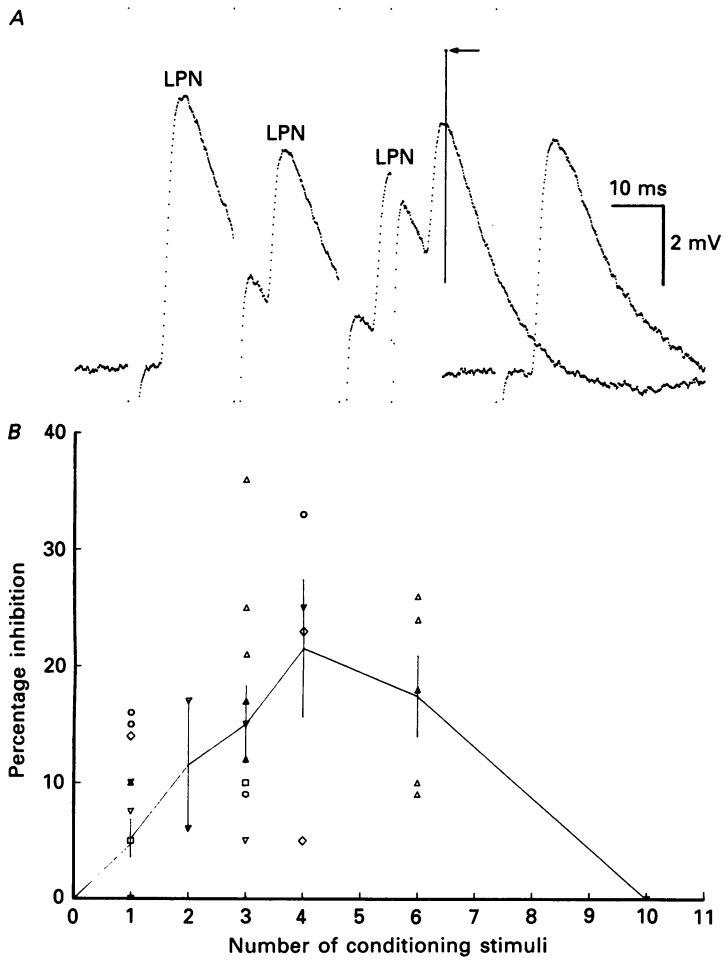

Fig. 12. Effect of multiple conditioning stimuli. *A*, three conditioning LPN responses were followed by a single SN response. The control SN response is displaced to the right for clarity. The arrow marks the peak of the control SN response, which is represented by the vertical line drawn rising from the extrapolated tail of the last conditioning response. *B*, summary of all results with multiple conditioning stimuli. Each symbol represents a different cell. Vertical lines show ± 1 S.D. In general, the amount of inhibition increased with the number of conditioning shocks. In the cell with ten conditioning stimuli, the amplitude of conditioning EPPs had decayed to a barely detectable level by about the seventh stimulus.

stimulating both nerves and stimulating the sural nerve (Both−SN in Fig. 5*B*). In other words, the upper trace in Fig. 8*B* is the amount added to SN by LPN when both nerves were stimulated simultaneously. Its rather flattened time course during the decay of the LPN response gives rise to the decay of inhibition during the EPC tail.

The decay of inhibition during the EPC tail could occur if, for some reason, large EPCs decayed more slowly than smaller EPCs. To check this possibility, the amplitude ratio SN/LPN was calculated for every point during SN and LPN EPCs; two of these ratios are plotted in Fig. 8 *C*. The upper curve is for the cell illustrated in Fig. 8*A* and *B*; the lower curve is from a different cell (Fig. 6*B*) in which SN was much smaller than LPN. The amplitude ratios declined slightly during the decay phases, but not enough to explain the observed decay of inhibition.

The decay of inhibition during the tail of the EPC suggests that the inhibition was active, although diminishing, during the time course of the test EPC. This suggests that it was not exclusively presynaptic in origin. Had it been presynaptic, one would predict that the inhibition would be constant during the decay phase (see Discussion).

Effect of holding potential on inhibition

Figure 9 shows the results of an experiment in which the amount of inhibition was measured in the same cell at membrane potentials of −40, −80 and −120 mV. Sample traces are shown in Fig. 9*A* and results with each response normalized to the average control amplitude at each holding potential are shown in Fig. 9*B*. There was no evident effect of muscle fibre holding potential on the magnitude of the inhibition. The experiment was performed in one other cell, with similar results.

ACh receptor block

In other experiments, signs of SN–LPN interaction were sought in preparations in which most ACh receptors were blocked. In one series, muscles were exposed to α-bungarotoxin for 10–20 min while monitoring EPPs in one fibre; when EPPs had been reduced to a low level, the preparation was perfused with normal Krebs solution. Because the postsynaptic responses were small, it was not necessary to voltage clamp the end-plate membrane; unclamped EPPs were recorded instead. We studied seventeen cells in this fashion (a total of eighty-one runs with varying stimulus protocols were obtained). In general the amount of inhibition was greatly reduced compared to unblocked preparations; about one-half of the cells showed negligible levels of inhibition. Overall, with single conditioning stimuli, the average inhibition of test EPPs was 15%; this was not significantly altered by correcting responses for non-linear summation of voltage. An example is shown in Fig. 10. Averaged EPPs are shown in Fig. 10*A*; the SN response which rose from the tail of the LPN EPP was about 20% smaller than expected (observed inhibition, 25%; after correction for non-linear voltage summation, 19%). As can be seen from Fig. 10*B*, this inhibition was nearly constant during the tail of the EPP. This is different from inhibition in unblocked preparations, which decayed during the decay of the test EPC. This might suggest that two inhibitory mechanisms operate, although the different recording conditions (voltage clamp in unblocked preparations, EPP recordings in α-bungarotoxin-treated preparations) must be taken into account (see Discussion).

Results from all α-bungarotoxin experiments in which single conditioning stimuli were used are shown in Fig. 11; the filled symbol is from the experiment illustrated in Fig. 10.

We performed a similar series of experiments in which *d*-tubocurarine, rather than

α-bungarotoxin, was used to block ACh receptors, with similar results. In twenty-seven cells studied (thirty-four runs in total), about half showed no significant inhibition; the average inhibition for all cells was 11%; the maximum was 32%.

Multiple conditioning shocks

In six cells treated with α-bungarotoxin, multiple conditioning shocks were delivered. An example is shown in Fig. 12*A*; three LPN conditioning stimuli were given, followed by a single SN test stimulus. The arrow marks the expected peak of the SN response. The vertical line was drawn to indicate the amplitude of the control SN response rising from the extrapolated tail of the last conditioning EPP. The test EPP was inhibited by about 35%. Non-linear voltage summation could account for only 4% of this inhibition (resting potential, −59 mV; reversal potential assumed to be −10 mV). The results from all six cells studied in this way are shown in Fig. 12*B*. It is clear that the amount of inhibition increased with two to six conditioning shocks. In one cell, the inhibition was absent when ten conditioning shocks were applied. In this cell, the ten conditioning EPPs sequentially declined in amplitude (depression); the tenth produced a barely detectable response.

In summary, the inhibition with postsynaptic blockade, while not observed in every cell with a single conditioning stimulus, appeared to be a real phenomenon. It could not be accounted for by non-linear summation, and it increased if several conditioning stimuli were given. Moreover, the inhibition did not decay during the tail of the EPP (in unblocked preparations the inhibition decayed during the decay of the test EPC).

DISCUSSION

Repetitive activity at chemically transmitting synapses is known to produce changes in the amplitude of successive synaptic potentials. In some cases, responses increase (facilitation, post-tetanic potentiation); in others responses decrease (synaptic depression). These changes have usually been attributed to presynaptic mechanisms such as intraterminal calcium accumulation (facilitation) or depletion of releasable vesicles (depression), which alter the amount of transmitter released. In the present study, conditioning stimulation produced a depression of test EPPs in neonatal rat lumbrical muscle (both stimuli delivered to the same nerve; see Fig. 3*A*).

Our main concern in this study was to look for *interaction* between inputs deriving from separate motoneurones but terminating at the same end-plate site on the muscle fibre in polyneuronally innervated neonatal muscles. We used the rat fourth deep lumbrical muscle because of its convenient dual nerve supply deriving from both the lateral plantar nerve (LPN) and the sural nerve (SN). We found clear evidence of time-dependent inhibitory interactions when measuring postsynaptic responses both as EPPs and, under voltage clamp, as EPCs. This is of interest because such interactions could be important in determining which neuromuscular contacts persist and which are lost in normal developmental synapse elimination. This is discussed further below.

The inhibitory interaction was reciprocal in that either nerve could inhibit the

other. Inhibition was greater with larger conditioning EPCs; for example, if the SN EPC was larger than the LPN EPC, then SN would inhibit LPN to a larger extent than LPN would inhibit SN. The inhibition was greatest if the conditioning and test responses were approximately superimposed. The longer the separation between conditioning and test stimuli, the less the inhibition; the total duration of the inhibitory effect was several tens of milliseconds, modestly longer than the duration of the EPC. Some possible explanations for these effects will now be considered.

Inadequate voltage clamp

If the voltage at the end-plate partially escaped clamping, the resulting end-plate potential would reduce the driving force for the subsequent test response, and so reduce the test EPC amplitude. This could occur either if clamp circuitry was inefficient or if the electrodes were not located precisely at the end-plate. The first possibility was routinely checked by measuring the membrane voltage (Fig. 2); at the peak of the EPC, if the driving force was reduced by more than about 3% the data were discarded. The second possibility (electrodes remote from end-plate) was also routinely checked in a number of ways, both optical and electrical. In some experiments, nerve terminals were stained with a fluorescent dye and electrodes were placed at the end-plate under visual guidance. Several electrical tests were also employed, including passive and active I–V curves with reversal potential, and comparison of time courses of EPCs and EPPs. These tests and other calculations, described in the Results and in the Appendix, strongly suggest that little voltage escape occurred at the end-plate. Moreover, the amount of escape needed to explain fully the observed inhibition was large, from 70 to 95% of the unclamped EPP. Taken together, these observations make it unlikely that technical artifacts like voltage escape could have produced the observed inhibition, and so we turned to a consideration of possible physiological mechanisms.

Presynaptic inhibition of transmitter release

Perhaps a substance released by the conditioning stimulus binds to the presynaptic membrane of the test nerve terminal, inhibiting its subsequent release. We tested for this possibility simply by extending measurements of inhibition from the peak of the test EPC to include the tail as well. If the inhibition were purely presynaptic, producing a reduction in the amount of transmitter released, then the amount of inhibition should remain constant throughout the duration of the test EPC. In fact, this was not the case; the inhibition decayed during the tail of the EPC (Fig. 12), suggesting that the mechanism responsible for the inhibition was on-going, although diminishing, during the conditioning EPC.

There are several ways in which this could conceivably occur, although the present experiments offer no direct evidence about such possibilities. One possibility is that the developing nerve terminals might interact electrically. Another is that ionic fluxes across nerve terminal membranes during the conditioning stimulus might alter ion concentrations in the vicinity of terminals active during the test stimulus. Such fluxes, however, would be far smaller than those that occur across the postsynaptic membrane in unblocked preparations. Finally, chemical substances released by the conditioning stimulus might directly interfere with transmitter release by the test

stimulus. Two substances known to be released by vertebrate motor nerve terminals are ACh and ATP (Schweitzer, 1987). Adenosine, a metabolite of ATP, has been shown to inhibit transmitter release (Silinsky, 1984; Silinsky, Ginsborg & Hirsh, 1987). Reports on the actions of ACh and its analogues have been conflicting, some reporting apparent enhancement, and others inhibition of release (Baldo & Van der Kloot, 1988; earlier work reviewed in Erulkar, 1983). If such substances act physiologically in an inhibitory fashion at neonatal terminals, their latency would have to be very short in order to explain the inhibition we have observed, suggesting, for example, a direct channel block rather than activation of a second messenger system.

Changes of concentrations of ions in the synaptic cleft

These could be brought about by the conditioning response. For example, flux of Na^+, Ca^{2+}, and K^+ through ACh-gated channels during the conditioning response could lead to depletion of Na^+ and Ca^{2+} and accumulation of K^+ in the synaptic cleft; this in turn could reduce both the amount of transmitter released by the test stimulus and the current through ACh-gated channels activated by the test EPC. The former would be a presynaptic effect, and as discussed above, cannot wholly explain the observed inhibition because the inhibition decayed during the tail of the test EPC. Reduction of postsynaptic current, on the other hand, might be relieved as cleft ions were replenished by diffusion from neighbouring extracellular fluid; thus the inhibition would decay during the tail of the test EPC, as observed. Depletion of cleft ions has been examined theoretically for the adult frog neuromuscular junction (Attwell & Iles, 1979). For a single spontaneous miniature EPC, the calculated changes in cleft Na^+ and K^+ concentration are large (30–40 % for each ion at the site of activated receptors), and the recovery of concentrations is only slightly slower than the time course of the decay of the EPC. Similarly, the inhibition we observed was large and decayed somewhat more slowly than the time course of the EPC. This mechanism, of course, would require that the conditioning response produce changes in the synaptic cleft at sites where the test response occurs.

Attwell & Iles (1979) also found that the calculated reversal potential was little altered as a result of altered cleft concentrations of sodium and potassium, owing to the approximately equal permeabilities of the channel to Na^+ and K^+. For example, as the membrane is clamped to more positive levels, the amount of Na^+ depletion in the cleft will be diminished, but this will be compensated for by an increased amount of K^+ accumulation in the cleft. Similarly, in two cells examined, we found that the amount of inhibition was about the same at -120, -80 and -40 mV. Thus, our results are consistent with a mechanism involving changes in ion concentrations in the synaptic cleft, which lead to a reduction in fluxes through ACh channels gated by the test stimulus.

Saturation of postsynaptic ACh receptors by the conditioning stimulus

If ACh released by conditioning and test stimuli partially share a common pool of receptors, and if these receptors are significantly saturated by the conditioning EPC, the test EPC would be reduced in amplitude. Moreover, one might predict that, as receptors become unbound during the conditioning EPC decay, the inhibition would decrease, as was observed. The inhibition should also be largely independent of

muscle fibre membrane potential, as observed. Lateral diffusion of ACh has been examined in detail by Hartzell, Kuffler & Yoshikami (1976) and Salpeter (1987). In adult animals, the action of acetylcholinesterase (AChE) severely curtails lateral diffusion of ACh, restricting receptor activation to the immediate vicinity of release. In neonates, however, where AChE activity may be less pronounced and where nerve terminals are very small and closely juxtapositioned, it is possible that terminals may partially share a common pool of receptors.

We tested for receptor saturation by examining synaptic interactions in preparations in which ACh receptors were partially blocked with curare or α-bungarotoxin. If receptor saturation were significant in unblocked preparations, then irreversibly blocking some receptors would have decreased the receptor pool size. Assuming constant fractional receptor occupancy, this should have produced no change in the amount of inhibition. If, on the other hand, partial blockade of receptors allowed more ACh to diffuse to neighbouring receptors, inhibition should have increased. In fact, the observed inhibition was decreased in receptor-blocked preparations: about one-half of the muscle fibres examined showed no inhibition, while the rest showed up to 40–50% inhibition. The overall mean was 15% inhibition. In six cells multiple conditioning stimuli were delivered, and the observed inhibition increased with the number of conditioning stimuli (unless the conditioning responses were greatly depressed; Fig. 12). Even with multiple conditioning stimuli, however, the inhibition in receptor-blocked preparations was less than in unblocked preparations. Thus, it is unlikely that receptor saturation accounts for the observed inhibition in unblocked preparations.

While ACh receptor blockade reduced the observed inhibition, it did not abolish it in every cell (Fig. 10). This inhibition, like that in unblocked preparations, was maximal when conditioning and test EPPs were approximately superimposed. Possibly, the inhibition in receptor-blocked preparations was simply a residuum of that observed in unblocked preparations. A further observation argues against this interpretation. As noted above, the inhibition in unblocked preparations decayed during the tail of the test EPC. In receptor-blocked preparations, on the other hand, the inhibition during the tail of the test EPP did not decay significantly (Fig. 10*B*), raising the possibility that two types of inhibition operate. This comparison must be viewed with caution, however, because EPPs, not EPCs, were recorded in receptor-blocked preparations, and even though EPPs were small, voltage-dependent changes such as charging of membrane capacitance could have obscured an underlying decay of inhibition during the EPP tail. Nevertheless, because of this difference in the decay of inhibition during the tail of the test response, other explanations were considered for the inhibition observed in receptor-blocked preparations. These experiments were not performed under voltage clamp conditions because the EPPs were only a few millivolts in amplitude. Correcting for non-linear voltage summation reduced the observed inhibition only slightly. Such corrections may in fact be unnecessary, since McLachlan & Martin (1981) showed that in adult mouse muscle no correction is necessary if EPPs are smaller than about 10 mV. It is possible that a voltage-sensitive postsynaptic conductance increase produced the reduction in test EPP amplitudes. However, such a conductance change would have to be highly sensitive to membrane potential and very fast to develop. In voltage clamp experiments, most fibres showed no significant change in

passive membrane properties with small depolarizations. Increases in membrane conductance with depolarization were seen in some fibres (Fig. 13, inset) but such changes required relatively large depolarizations and developed too slowly to account for the inhibition observed in receptor-blocked preparations.

Implications for synapse elimination

During the neonatal period, nerve terminals from different axons compete with each other for sole occupancy of the end-plate. By about 3 weeks of age, each end-plate is innervated by only one motor axon, all others having been eliminated. Similar events occur in adult muscle during reinnervation after nerve crush. There is evidence that synapse elimination in the rat lumbrical muscle is based partly on the level of electrical activity in motor axons, with more active nerve terminals at a competitive advantage (Ribchester & Taxt, 1983; 1984; Ridge & Betz, 1984; Ribchester, 1988; reviewed in Betz, 1987; and Ridge, 1989; but see Callaway, Soha & Van Essen, 1987). The cellular mechanisms by which activity exerts its influence are not known. It is natural to enquire whether the inhibitory interactions described in this paper play a role in this process. For example, one model of competitive synapse elimination is that postsynaptic receptor activation causes local release by the muscle fibre at that site of a trophic substance which nerve terminals require for synapse stabilization; its uptake by the terminals, perhaps in conjunction with vesicle recycling, is dependent upon recent nerve activity. Thus, according to this model, inhibition of transmitter release and/or inhibition of transmitter action might lead to a decreased capacity to take up trophic substance. In attempting to apply the present results to this model, several apparently severe constraints arise. One constraint is temporal – the inhibition we observed lasts only a few tens of milliseconds. This imposes severe restrictions on the rate and pattern of activity in convergent axons, if this were to play a role in synapse elimination. Interestingly (although its physiological significance is not known), presynaptic inhibition at the crayfish neuromuscular junction lasts only about 5–8 ms (Dudel & Kuffler, 1961). Another constraint is spatial. The mechanisms of inhibition we have considered operate only over small distances, in the order of several micrometres; virtually direct nerve terminal apposition is required. Lichtman *et al.* (1985) have shown that in embryonic snake fast twitch muscles, synaptic boutons from different neurones do interdigitate in a fashion that might promote such short-range interactions. Whether such intimate contact occurs in mammals is not known; electron micrographs (Bixby, 1981) show nerve terminal profiles in direct contact, but it is not known which profiles belong to which neurones. Clearly, it would be of interest to know more about the spatial distribution of terminals belonging to different motoneurones at single end-plates in mammalian muscle.

APPENDIX

Quantitative tests of voltage clamp efficiency

After an experiment was completed we performed further tests to check that impalements were at the end-plate; if not, the data were discarded. The *I–V* relationship for the cell illustrated in Fig. 5 is shown in Fig. 13. The passive *I–V* curve

is plotted in Fig. 13*A*; measurements were taken 1 ms before the EPC deflections (inset). The input slope conductance increased (with a delay) approximately 12-fold between −90 and +5 mV, from 50 to 640 nS. EPC amplitudes are plotted against membrane potential in Fig. 13*B*; the reversal potential is −10 mV and the

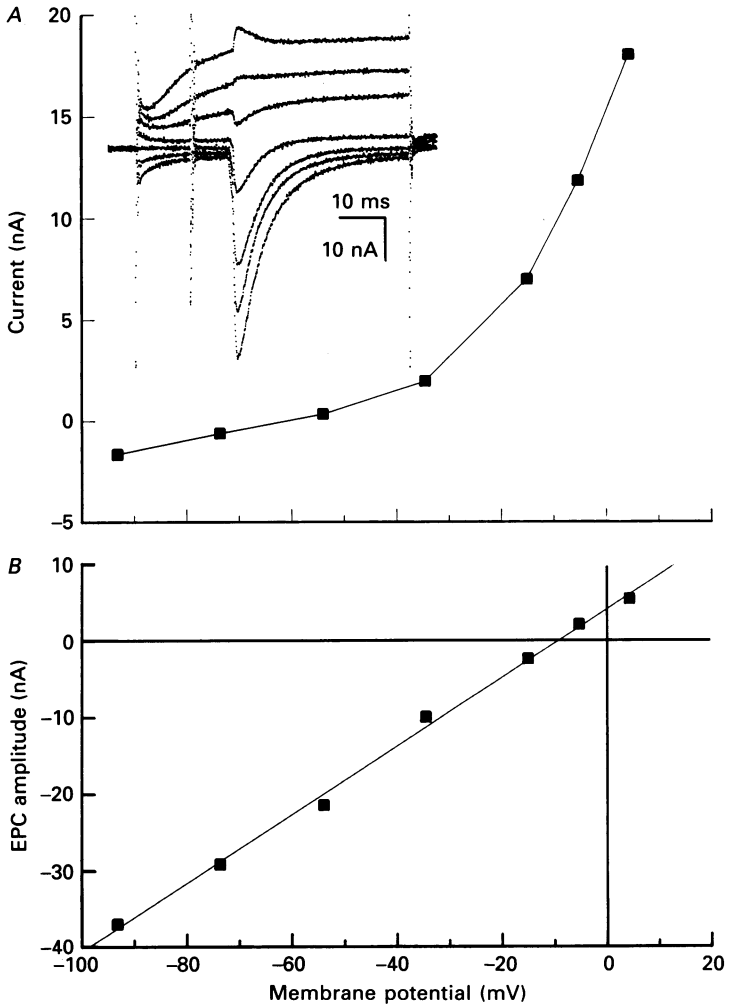

Fig. 13. *I–V* curve for cell illustrated in Figs 6, 8 and 9. *A*, passive membrane properties measured 1 ms before the start of EPC (see inset traces). Input conductance increased more than 30-fold between −90 and +5 mV. *B*, EPC amplitudes at different membrane potentials. The reversal potential was −10 mV. The line is the best linear fit to the points. The negative reversal potential and linear EPC–membrane potential relationship in the face of a highly rectifying membrane suggests that the end-plate was well clamped.

relationship is reasonably linear throughout the entire voltage range. This linearity in the face of highly rectifying passive membrane properties and the negative reversal potential further suggests that the impalements were very close to the end-plate. If the impalements had been remote from the end-plate, the clamp efficiency would have deteriorated with membrane depolarization, owing to the fibre's greatly

shortened length constant at depolarized potentials. This would have led to increased voltage escape at the end-plate, shifting the measured reversal potential in a positive direction and curving the relationship in Fig. 10*B* (concave downward).

We next estimated the maximum distance from the end-plate possible, given the

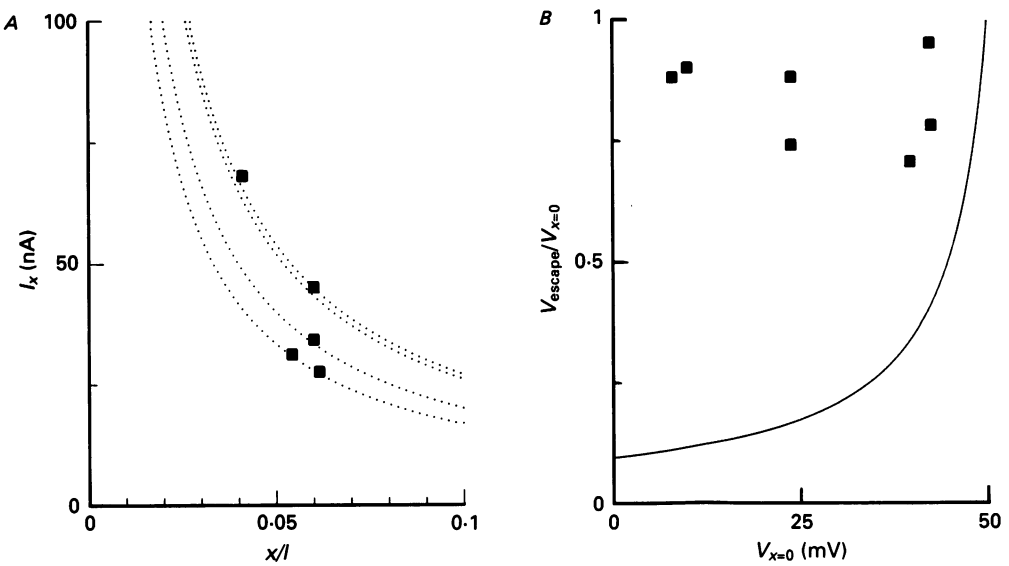

Fig. 14. Electrical estimates of distance between clamp electrodes and end-plates. *A*, curves show theoretical current I_x (see text for equation) as a function of distance from end-plate, based on an extreme assumption (ACh action causes a complete short circuit at the end-plate). Squares mark observed currents and give an upper limit (about 0·06 space constants) to the distance from end-plate. There are multiple curves because runs were carried out at slightly different holding potentials. *B*, assuming that clamp electrodes were 0·06 space constants from the end-plate, the line plots the theoretical relationship between the fractional voltage escape at the end-plate and the size of the unclamped EPP. The squares mark the escape which would be required to explain the observed inhibition (cf. Fig. 7). The poor agreement is further evidence that the inhibition cannot be explained by voltage escape at the end-plate.

observed EPC amplitudes and muscle fibre input resistance. That is, we made the worst case assumption that ACh action at the end-plate produced a short circuit, reducing the input resistance to zero at that site. With the electrodes at the end-plate, this would produce an infinitely large EPC. Figure 14*A* shows the expected relationship between EPC amplitude (I_x) and electrical distance (x/l) from the end-plate, where x is distance between end-plate and clamping electrodes and l is the length constant. The squares mark the observed currents on the appropriate curve. (There is more than one curve because different runs were carried out at slightly different holding potentials.) The lines were calculated as follows; the total current (I_{tot}) flowing at an end-plate with remote clamping electrodes is given by Auerbach & Betz (1971, eqn (4)) as:

$$I_{tot} = \frac{V_0}{R_s + 2R_0/(1+\coth(x/l))},$$

where R_s = synaptic resistance due to ACh action and R_0 = input resistance, V_0 =

driving force (membrane potential − reversal potential), x = distance between end-plate and clamping electrodes, and l = length constant. I_{tot} divides into two components: one passes along the muscle fibre towards the clamp electrodes ($I_>$) and the other away from the clamp electrodes. The amount passing towards the electrodes is given by:

$$I_> = I_{tot}/(1+\tanh(x/l)).$$

Part of this current leaks out of the fibre before reaching the clamp electrodes; the current reaching the electrodes (I_x) is given by:

$$I_x = I_>/\cosh(x/l).$$

The lines in Fig. 14*A* were drawn according to this equation. R_0 was measured directly; reversal potential was assumed to be -10 mV; R_s was set to zero (short circuit at end-plate). These calculations are based on several assumptions, namely, perfect clamping efficiency and complete charging of membrane capacitance between clamp elecrodes and end-plate. Errors arising from these assumptions are probably small; the observed clamping efficiency was over 97% and the distances being considered are a small fraction of a length constant, making it likely that capacitative lags were negligible.

None of the squares in Fig. 14*A* is at a distance greater than about 0·06 length constants from the end-plate. This, of course, is an upper limit, since the transmitter action at the end-plate was assumed to be infinite.

In another test, SN and LPN EPP and EPC amplitudes were used to predict reversal potential. Assuming that electrodes are located at the end-plate, EPP amplitude V is given by:

$$V = V_0 R_0/(R_0+R_s),$$

and EPC amplitude I by:

$$I = V_0/R_s.$$

Combining these two equations, and solving for R_0 gives:

$$R_0 = V V_0/I(V_0-V).$$

Adding subscripts for sural nerve (SN) and lateral plantar nerve (LPN) responses and solving for V_0 gives:

$$V_0 = V_{SN}(I_{SN}/I_{LPN}-1)/(I_{SN}/I_{LPN}-V_{SN}/V_{LPN}).$$

The reversal potential is simply the resting potential $+V_0$. For the cell in Fig. 14, the reversal potential calculated from this relationship is -9 mV, close to the measured value (-10 mV). More generally, one can ask how the measured reversal potential (E_{rev}) changes with distance from the end-plate. At EPC reversal, the error in measuring E_{rev} is simply the difference between the membrane potential at the recording site and at the end-plate ($V_x - E_{rev}$), which is given by:

$$(E_{rev}-RP)(e^{x/l}-1),$$

where RP = resting potential. With RP = -60 mV, the error is about 11 mV when

$x/l = 0{\cdot}2$. This is misleading, however, because in the cell in Fig. 14, the input resistance fell by about an order of magnitude when the cell was depolarized to about -10 mV. Since length constant is proportional to input resistance, 0·2 length constants at -10 mV is equivalent to approximately 0·02 length constants at -60 mV. In other words, if the electrodes had been more than a few hundredths of a length constant (measured at the resting potential) away from the end-plate, the error in estimating the reversal potential would have been more than 10 mV. This would have required that the true reversal potential be more negative than -20 mV, which is very unlikely.

In summary, the results taken together make it seem reasonable to conclude that the impalements were within 0·06 length constants of the end-plate. In a final calculation, we used this value to estimate the maximum amount of voltage escape that might have occurred in this cell; results are shown in Fig. 14*B*. The squares show the escape that would be required to explain the observed inhibition (cf. Fig. 7). The line shows the escape expected as a function of EPP amplitude, assuming that the clamp electrodes were 0·06 length constants from the end-plate (calculated according to Auerbach & Betz, 1971, eqn (6)). It is clear that voltage escape cannot account fully for the observed inhibition. One can add further that, if the apparent inhibition were due solely to voltage escape, we should have recorded from the occasional cell which, impaled precisely at the end-plate, showed no inhibition. In fact, in voltage clamp experiments on unblocked preparations, all cells showed an inhibitory effect.

Supported by research grants from NIH (NS23466 to W.J.B. & R.M.A.P.R.) and MDA (to W.J.B.) and by a Fellowship from MDA (to M.C.). We gratefully acknowledge the unfailing technical assistance of Mr Steven Fadul.

REFERENCES

ATTWELL, D. & ILES, J. F. (1979). Synaptic transmission: ion concentration changes in the synaptic cleft. *Proceedings of the Royal Society* B **206**, 115–131.

AUERBACH, A. & BETZ, W. J. (1971). Does curare affect transmitter release? *Journal of Physiology* **213**, 691–705.

BALDO, G. J. & VAN DER KLOOT, W. (1988). Transient elevation of spontaneous release at the frog neuromuscular junction following acetylcholine iontophoresis. *Pflügers Archiv* **411**, 188–194.

BETZ, W. J. (1987). Motoneurone death and synapse elimination in vertebrates. In *The Vertebrate Neuromuscular Junction*, ed. SALPETER, M. M., pp. 117–162. New York: Alan R. Liss.

BETZ, W. J., CALDWELL, J. H. & RIBCHESTER, R. R. (1979). The size of motor units during post-natal development of rat lumbrical muscle. *Journal of Physiology* **297**, 463–478.

BETZ, W. J., CHUA, M. & RIDGE, R. M. A. P. (1989). Inhibitory interactions between motoneurone terminals at neonatal rat neuromuscular junctions. In *Neuromuscular Junction*, Fernström foundation series 13, ed. SELLIN, L. C., LIBELIUS, R. & THESLEFF, S., p. 582. Amsterdam: Elsevier.

BIXBY, J. L. (1981). Ultrastructural observations on synapse elimination in neonatal rabbit skeletal muscle. *Journal of Neurocytology* **10**, 81–100.

CALLAWAY, E. M., SOHA, J. M. & VAN ESSEN, D. C. (1987). Competition favouring inactive over active motor neurones during synapse elimination. *Nature* **328**, 422–426.

DUDEL, J. & KUFFLER, S. W. (1961). Presynaptic inhibition at the crayfish neuromuscular junction. *Journal of Physiology* **155**, 543–562.

ERULKAR, S. D. (1983). The modulation of neurotransmitter release at synaptic junctions. *Reviews of Physiology, Biochemistry and Pharmacology* **98**, 63–175.

HARTZELL, H. C., KUFFLER, S. W. & YOSHIKAMI, D. (1976). The number of acetylcholine molecules

in a quantum and the interaction between quanta at the subsynaptic membrane of the skeletal neuromuscular junction. *Cold Spring Harbor Symposia on Quantitative Biology* **40**, 175–186.

LICHTMAN, J. W., WILKINSON, R. S. & RICH, M. M. (1985). Multiple innervation of tonic endplates revealed by activity-dependent uptake of fluorescent probes. *Nature* **314**, 357–359.

MCLACHLAN, E. M. & MARTIN, A. R. (1981). Non-linear summation of end-plate potentials in the frog and mouse. *Journal of Physiology* **311**, 307–324.

MAGRASSI, L., PURVES, D. & LICHTMAN, J. W. (1987). Fluorescent probes that stain living nerve terminals. *Journal of Neuroscience* **7**, 1207–1214.

RIBCHESTER, R. R. (1988). Activity-dependent and -independent synaptic interactions during reinnervation of partially denervated rat muscle. *Journal of Physiology* **401**, 53–75.

RIBCHESTER, R. R. & TAXT, T. (1983). Motor unit size and synaptic competition in rat lumbrical muscles reinnervated by active and inactive motor axons. *Journal of Physiology* **344**, 89–111.

RIBCHESTER, R. R. & TAXT, T. (1984). Repression of inactive nerve terminals in partially denervated rat muscle after regeneration of active motor axons. *Journal of Physiology* **347**, 497–511.

RIDGE, R. M. A. P. & BETZ, W. J. (1984). The effect of selective, chronic stimulation on motor unit size in developing rat muscle. *Journal of Neuroscience*. **4**, 2614–2620.

RIDGE, R. M. A. P. (1989). Competition and activity during developmental synapse elimination in skeletal muscle. In *Neuromuscular Stimulation: Basic Concepts and Clinical Applications*, ed. CLIFFORD ROSE, F., JONES, R. & VRBOVA, G. New York: Demos (in the Press.)

SALPETER, M. M. (1987). Vertebrate neuromuscular junctions: General morphology, molecular organization, and functional consequences. In *The Vertebrate Neuromuscular Junction*, ed. SALPETER, M. M., pp. 1–54. New York: Alan R. Liss.

SCHWEITZER, E. (1987). Coordinated release of ATP and ACh from cholinergic synaptosomes and its inhibition by calmodulin antagonists. *Journal of Neuroscience* **7**, 2948–2956.

SILINSKY, E. M. (1984). On the mechanism by which adenosine receptor activation inhibits the release of acetylcholine from motor nerve endings. *Journal of Physiology* **346**, 243–256.

SILINSKY, E. M., GINSBORG, B. L. & HIRSH, J. K. (1987). Modulation of neurotransmitter release by adenosine and ATP. *Progress in Clinical and Biological Research* **230**, 65–75.

WERLE, M. J. & HERRERA, A. A. (1987). Synaptic competition and the persistence of polyneuronal innervation at frog neuromuscular junctions. *Journal of Neurobiology* **18**, 375–389.